Earth Surf. Dynam. Discuss., 3, 53–82, 2015
www.earth-surf-dynam-discuss.net/3/53/2015/
doi:10.5194/esurfd-3-53-2015
© Author(s) 2015. CC Attribution 3.0 License.

Earth Surface Dynamics
Discussions
Open Access

This discussion paper is/has been under review for the journal Earth Surface Dynamics (ESurfD). Please refer to the corresponding final paper in ESurf if available.

# Bedload transport controls intra-event bedrock erosion

**A. R. Beer**[1,2] **and J. M. Turowski**[1,3]

[1]Swiss Federal Institute for Forest, Snow and Landscape Research WSL, Mountain Hydrology and Mass Movements, Zürcherstrasse 111, 8903 Birmensdorf, Switzerland
[2]Swiss Federal Institute of Technology ETH Zurich, Department of Environmental System Science, 8092 Zürich, Switzerland
[3]German Research Centre for Geosciences GFZ, Section 5.1, Telegrafenberg, 14473 Potsdam, Germany

Received: 2 December 2014 – Accepted: 8 December 2014 – Published: 6 January 2015

Correspondence to: A. R. Beer (alexander.beer@wsl.ch)

Published by Copernicus Publications on behalf of the European Geosciences Union.

## Abstract

Fluvial bedrock incision constrains the pace of mountainous landscape evolution. Fluvial erosion processes have been described with incision models that are widely applied in river reach and catchment scale studies. However, so far, no linked field data set at the process scale had been published that allows to assess model requirements and adequacy. Here, we evaluate the predictive power of various incision models on data on hydraulics, bedload transport and erosion recorded on an artificial bedrock slab installed in a steep mountain stream for a single bedload transport event. The influence of transported bedload on erosion rate (the "tools effect") is shown to be dominant while other effects are of minor importance. Hence, a simple temporal distributed incision model in which erosion rate is proportional to bedload transport rate is proposed for transient local studies. This model can be site-calibrated with temporally lumped bedload and erosion data and its applicability can be assessed by visual inspection of the study site. Basic discharge-based models like derivatives of the stream power model family however, are adequate to reproduce the overall trend of the observed erosion rate, at least for the event on hand. This is relevant for long-term studies of e.g. landscape evolution with no interest in transient local behaviour.

## 1 Introduction

Quantitative landscape evolution analysis is a fundamental domain of today's geomorphological research. The hydrological system plays an important role in landscape response to tectonics by the formation of drainage networks, adjustment of river channel shape and slope, and by routing sediments (e.g. Howard et al., 1994; Whipple and Tucker, 1999; Whipple, 2004). Thus, a mechanistic understanding of the processes active in rivers and their mathematical description is crucial for capturing landscape evolution as a whole (e.g. Lague, 2014). Bedrock rivers are particularly frequent in mountainous regions and there have been many efforts to model their erosional work

cc BY

(overviews by Sklar and Dietrich, 2006; Turowski, 2012; Whipple et al., 2013). A number of physical fluvial erosion processes acting on bedrock surfaces have been described, and abrasion by bedload and plucking of blocks are thought to be the most important of these (cf. Whipple et al., 2013). Both of these are driven by the impact of bedload particles.

Bedrock incision is generally thought to depend on flow hydraulics and in-situ substrate properties. This notion forms the basis of the most commonly used erosion models of the stream power incision model family (Howard and Kerby, 1983; Seidl et al., 1994; Turowski, 2012; Lague, 2014), in which erosion rate is a power function of stream power or bed shear stress (Whipple and Tucker, 1999). However, mechanistically, it is known that fluvial bedrock incision is driven by the impact of sediment particles (Sklar and Dietrich, 2001; Hartshorn et al., 2002; Turowski, 2012; Cook et al., 2013). Several effects due to the transported sediment need to be accounted for. These are "thresholds of motion and suspension" relating to a characteristic grain size (Lague et al., 2003; Sklar and Dietrich, 2004; Attal et al., 2011), the shielding of bedrock by sediments, known as the "cover effect" (e.g., Gilbert, 1877; Turowski et al., 2008; Johnson et al., 2009), and erosive pebble impacts on the bedrock that depend on the amount of mobile sediment, known as the "tools effect" (e.g., Foley, 1980; Turowski and Rickenmann, 2009; Cook et al., 2013). Taking into account these four effects, erosion rate $E$ can be written as (cf. Sklar and Dietrich, 2006):

$$E = K H_y^a S_e^b F_e^c Q_s^d \tag{1}$$

Here, the scaling of bedrock erodibility, sediment erosivity and thus the dominant erosional process is lumped in a model-specific prefactor $K$ (e.g., Howard, 1994; Sklar and Dietrich, 2006). $H_y$ is a placeholder for an effective hydraulic parameter (e.g., discharge, stream power, bed shear stress) incorporating the grain motion threshold. The suspension effect term $S_e$ regulates the fraction of particles in suspension, $F_e$ describes the cover effect, and $Q_s$ is the sediment transport rate, describing the availability of ero-

CC BY

sive tools (see Appendix A for more details). The exponents $a$, $b$, $c$, and $d$ modulate the dependence of erosion rate on these four effects, respectively.

Available fluvial erosion models were originally developed at the process scale, and their application to whole stream sections or even catchments is problematic (e.g. Lague et al., 2005). Spatial upscaling from process to reach scale and from reach to catchment scale is incompletely understood. Factors such as time (Gardner et al., 1987; Mills, 2000; Finnegan et al., 2014), space (Hancock et al., 1998; Wohl, 1998; Goode and Wohl, 2010), and variability in forcing conditions, e.g., discharge, climate or sediment process interactions (Hancock et al., 1998; Snyder et al., 2003; Lague et al., 2005; Whipple et al., 2013), need to be taken into account explicitly. In addition, many models predict similar steady-state morphology (e.g., Whipple and Tucker, 2002; Lague, 2014), but the transient evolution of entire channels is difficult to reconstruct in the field, and hence model validation is challenging.

Theoretical considerations of incision model sensitivity (Sklar and Dietrich, 2006) and model assessment by means of field data so far have largely focused on the steady state geometry of entire channels (Lague, 2014). Van der Beek and Bishop (2003) remodelled the long-profile evolution of incising rivers in the Upper Lachlan catchment (SE Australia) based on known paleo-profiles. They found that all of the tested models gave reasonable predictions for the current long profiles with the application of suitable parameter sets. In contrast, Tomkin et al. (2003) determined that none of the tested models could satisfactorily explain their data of the well-studied Clearwater River (NW Washington State, USA), which is thought to exhibit steady state incision. Tomkin et al. (2003), however, attributed this failure more to the quality of their data, rather than to the inadequacy of the applied incision models. A different approach was taken by Turowski et al. (2013), who compared field measurements of energy delivery to the stream bed to predictions using the saltation-abrasion model (Sklar and Dietrich, 2004). However, since only one element of several constituting this model was compared to data, this approach can only be applied to specific model types.

The problem of model adequacy and potential study-site sensitivity can be simplified if models and their behaviour were examined at the process scale (Whipple and Tucker, 1999; Tucker and Whipple, 2002). However, such an evaluation has not been possible so far due to the lack of highly resolved data (Turowski, 2012), and the transient validity of fluvial erosion models at the process scale has neither been assessed in the laboratory nor in the field. Here, we use field data of unprecedented detail and quality (Beer et al., 2014) to directly evaluate available fluvial incision models at the process scale, using a transient erosional signal throughout a single sediment transport event. Thus, we obtain constraints for the modelling of fluvial bedrock erosion at a scale that has not previously been studied.

## 2 Observation site and data

The Erlenbach is a small pre-alpine mountain stream in Switzerland that hosts a well-instrumented bedload transport observatory. In 2011 the site has been supplemented with a novel setup for measuring bedrock erosion. Infrastructure, measurement methods and accuracy have been described in detail elsewhere (Rickenmann et al., 2012; Turowski et al., 2013; Beer et al., 2014), and are only briefly summarised here. Discharge is gauged with 15 % uncertainty, bedload mass transport (in the following referred to as bedload transport) can be determined to 1 kg with 30 % uncertainty using the Swiss plate bedload sensor system, and at-a-point erosion sensors have a resolution of better than 0.1 mm with 5 % uncertainty (Beer et al., 2014). The measurements of these three quantities are completely independent and all data are recorded at minute resolution.

For the following analysis we study a rainfall-induced discharge event, featuring a peak flow of 1.13 $\mathrm{m^3\,s^{-1}}$ (Beer et al., 2014). The period of investigation is set from the onset of the stream's response to rainfall and ends some hours after the rainfall, broadly enclosing the actual bedload transport event. We focus on the surface erosion measured on a dry-packed concrete slab (a test "bedrock") installed flush with the streambed that was overpassed by 8.8 t of bedload in nearly 11 h, as detected by a geophone sensor located immediately downstream (Rickenmann et al., 2012; Beer et al., 2014). This slab hosted three vertical at-a-point erosion sensors that continuously record surface elevation. In addition, it was surveyed with photogrammetry (Rieke-Zapp et al., 2012) before and after the event to confirm the measured cumulative erosion rates at the positions of the erosion sensors.

Here, we restrict our analysis to erosion sensor c3, which is located in the middle of the flow path and features the highest erosion rate (cf. Beer et al., 2014). The sensor recorded 13 erosion steps during the event, with a total erosion of 0.85 mm. The temporal evolution of erosion until the first recorded step is unknown, hence only the subsequent data are used for analysis. To account for the temporal uncertainty of the occurrence of the individual erosion steps and to obtain a transient curve, we use linearly interpolated data, in the following referred to as c3i. The course of this curve robustly represents the erosional evolution of the surrounding slab surface (cf. Beer et al., 2014).

## 3 Methods

Sklar and Dietrich (2006) classified the spectrum of existing incision models according to their incorporation of the four types of sediment effects (Eq. 1). We selected a representative of each of their classes (Table 1). These models are (i) unit stream power (USP), (ii) excess unit stream power (EUSP), (iii) linear decline (LD), (iv) alluvial bedload (AB), (v) tools (T), (vi) parabolic stream power (SPP), and the saltation-abrasion model (vii) without (SAws) and (viii) with the suspension effect (SA). In addition, we included a variant of T, a tools-only dependent model (TO), in which erosion rate is proportional to cumulated bedload transport rate (see Appendix A for model details). A model based on stream power can be converted into a model based on shear stress and vice versa using simple assumptions on hydraulic geometry and flow velocity (e.g.,

CC BY

Whipple and Tucker, 1999). Thus, the models USP and EUSP can be seen to be representative for other members of the stream power model family.

We calculated erosion rates with each model for the considered flood event using independently observed hydraulic parameters and sediment transport rates. The relations between discharge, flow height and water table width that are required for calculation of hydraulic parameters such as local unit stream power at the position of the observed bedrock slab were constructed using the methods described by Beer et al. (2014). The mean grain size of transported sediment during the event considered here was estimated at 0.02 m (using data by Rickenmann et al., 2012, Fig. 9) at a mean discharge of $0.77\,\mathrm{m^3\,s^{-1}}$ and a mean bedload transport rate of $0.45\,\mathrm{kg\,m^{-1}\,s^{-1}}$ for the period of observed bedload transport. During the event, bedrock abrasion was apparently the dominant erosional process, since indications for solution, plucking or cavitation were neither given by direct observation nor by surveying results (Beer et al., 2014).

The threshold of bedload motion here was defined at the observed exceedance of a bedload transport rate of $1\,\mathrm{kg\,min^{-1}}$ at the beginning of the event, corresponding to a discharge of $0.36\,\mathrm{m\,s^{-1}}$ and a unit stream power of $407\,\mathrm{W\,(m^2)^{-1}}$. This corresponds to a critical shields stress of 0.26, 2.7 times higher than a threshold estimated by an empirical equation for steep streams (cf. Lamb et al., 2008b, Fig. 1). However, we focus on continuous bedload transport likely affecting the entire stream width. The interpolated erosion line c3i and the individual model outcomes were scaled to one to focus on transient behaviour, ignoring the prefactors $K$ with their multivariate sensitivities to lithology, climate and sediment (Whipple and Tucker, 1999).

Model sensitivity on bedload transport was assessed using three separate simulation time periods. For the “long period”, start and end of the simulation were set at arbitrary times before and after the observed bedload transport event. In the “bedload period”, start and end of the simulation period coincide with the observed bedload transport period, and the “erosion period” only covers the time span where c3i data exists.

Overall deviations between model predictions and c3i were quantified by the root mean square error (RMSE, cf. van der Beek and Bishop, 2003; Valla et al., 2010) and minute-by-minute deviations were considered to assess model feasibility and highlight dominant processes. In addition, we optimized individual model performance by adjusting the exponents *a*, *b*, *c*, and *d* (see Eq. 1), as long as they differed from zero, to minimize the RMSE based on the methods of Brent (1973) and Nelder and Mead (1965).

## 4 Results

The applied incision models can be roughly separated into two groups based on their transient behaviour, corresponding to those models that do and those that do not include the tools effect $Q_s$ (Fig. 1, Table 1). Here, we focus on the long period to describe the main observations. A detailed comparison for each model in each time period is given in Appendix B (Fig. A1).

The models of the first group (models classes I–IV; Fig. 1a; Table 1) display a smooth increase of erosion over the course of the event, while those of the second group (model classes Va–VIII; Fig. 1b) display a wavy pattern. With respect to the four sediment effects, we observed the following:

i. Threshold of motion: the timing of bedload transport is of distinct importance, especially if the tools effect is ignored in addition to the threshold, since models neglecting both effects (USP and LD) predict erosion even when none was detected (cf. Sklar and Dietrich, 2006). This is particularly obvious for the end of the observation period (Fig. 1a and c).

ii. Threshold of suspension: the status of complete suspension transport (this would correspond to $S_e = 0$; see Appendix A) was not reached during this event for grain sizes equal or greater than 0.02 m (cf. Fig. 1c). The mean of the suspension term $S_e$ was $0.64 \pm 0.18$ throughout the event, with a minimum of 0.34, and thus substantial pebble saltation was predicted. The use of model SA that includes the suspension effect term showed a larger deviation from the data than the otherwise equal model SAws (Fig. 1b).

iii. Cover effect: the cover term $F_e$ averaged at 0.91 ± 0.13, and there was negligible time of full bed cover calculated during which erosion was completely prohibited (0.1 % with $F_e = 0$; Fig. 1c). Thus, there is no remarkable improvement when including the cover term when comparing for example models USP and LD (Fig. 1a).

iv. Tools effect: the wavy pattern observed in the erosion record c3i as well as in the models including the tools effect (TO to SA; Fig. 1b) closely follows the evolution of cumulative bedload transport $Q_{s,cum}$ over the course of the event with model SPP showing the largest deviation. Actual bedload transport $Q_s$ initiates at the threshold of motion by definition here (cf. Fig. 1c and methods). However, it recedes before falling below this threshold again at the end of the observation period. The latter is in agreement with the evolution of c3i.

Models including the tools effect (model classes Va to VIII) show smaller RMSE than those that do not for all three time periods, except model SPP charged with the standard parameters (Table 2). All model predictions except for model TO improved when optimized, with the highest improvements for the erosion period. However, for model SA the optimized exponents of both threshold factors (motion and suspension) show implausible values. For all other models, exponents only adjusted moderately during optimization.

Analysis of the minute-by-minute deviations of each model prediction from c3i reveals the same pattern for all three simulation periods: model predictions are generally better when the tools effect, represented by $Q_s$, is included (Fig. 2). Generally the long period and the bedload period featured similar results, while for the erosion period, models showed comparably worse predictions. Models neglecting $Q_s$ underpredicted observed erosion on average by around 9 % for the first two periods, models including the tools effect only deviated by 0.4 % (cf. Fig. 1a and b for the erosion period 4 %).

The interquartile ranges show a similar pattern, with models SAws and SA giving the smallest values when using the optimized parameter sets, but their overall performance is comparable to the TO model. Model SPP, which neglects the threshold of motion, shows the worst performance of all approaches considering bedload tools, when standard parameters are used. Model parameter optimization achieved most enhancement for the erosion period, where the performance of models including $Q_s$ could be improved to a comparable quality as in the two other periods using standard parameter sets.

## 5 Discussion

### 5.1 Model sensitivity on time period

Incision model behaviour was comparable for the long period and the bedload period, but for the erosion period the performance of all models was notably worse (Fig. A1). However, the latter is an artefact of scaling all erosion series to one for the evaluation. In contrast to both of the other periods, in which bedload transport and erosion actually started within the time period of consideration, analysis for the erosion period began with c3i set to 0 to assure a common initiation of all variables. Thus, any erosion that occurred before the beginning of the erosion period was disregarded. With $R^2 = 0.96$, the strength of the correlation between c3i and the cumulative bedload $Q_{s,cum}$ during the erosion period is a little smaller than for the long period and the bedload period ($R^2 = 0.98$ for both), and this smaller correlation translates directly to the predictive power of the tools effect for measured erosion. The decreased correlation strength may be due to various reasons: (i) if the bedload path in the channel bed systematically changes as discharge increases, the correlation between bedload transport rates and erosion rates may decrease, as small discharges have been omitted in the erosion period. (ii) Bedload transport rates are measured over the entire slab surface (0.18 m$^2$), but the erosion sensor records at a point. (iii) The erosion sensor does not measure continuously, but in steps. Therefore, temporal variability in pebble impacts can cause mismatches between bedload transport rates and erosion rates. (iv) Due to the shorter period of interest, and to the scaling of the total erosion rate to one, the sharp increase of c3i around 05:40 (Fig. 1) resulted in higher relative deviations of the incision models.

Nevertheless, the pattern observed for the relevance of the sediment effects remains the same for all periods. In addition, the RMSE values are reasonably similar for all three time periods both for the common and the optimized model versions. Hence, at least for the time scales investigated here, there is no significant temporal sensitivity for model application regarding actual bedload transport.

## 5.2 Relevance of the sediment effects

In the following we evaluate the predictive power of the four sediment effects by means of the long period. The inclusion of a threshold of bedload motion limits the prediction of erosion to the time when hydraulic conditions exceed this threshold. With a suitable choice of threshold, a good match with the observations can be obtained. Even though the details in the transient pattern of erosion cannot be reproduced with models EUSP and AB, the inclusion of the threshold allows the prediction of the general observed trend at least for this event. Thus, as has been previously suggested (Lague et al., 2003; Chatanantavet et al., 2013; Lague, 2014), the inclusion of a threshold is necessary to obtain a plausible temporal pattern of erosion. Therefore, if no direct information on bedload transport is available, the threshold of motion in $H_y$ might be the most relevant parameter for erosion modelling (cf. Sklar and Dietrich, 2006; Attal et al., 2011).

Within the data analysed here, the inclusion of the suspension effect term did not substantially change predictions in comparison to otherwise equal models that did not include it. Applying a suspension threshold of 3 instead of 1 in the suspension effect term $S_\mathrm{e}$ (see Appendix A) did not change the predictions of the SA model. A lower threshold value (0.5) caused premature erosion at low shear stresses and prohibited erosion at high shear stresses. During the event, the ratio of active over critical

cc BY

shear stress had a mean value of 1.72 and a maximal value of 3.15 for the studied grain size of 0.02 m. Therefore we did not separately apply the incision model of Lamb et al. (2008a) that specifically addresses abrasion by particles in the suspension regime, since this model only differs from the SA model for shear stress ratios exceeding 10 (Lamb et al., 2008a). The bedload regime prevailed and the erosional contribution of bedload transport was dominant over the one of suspended load. The slightly better performance of the SAws model compared to the SA model can be assigned to the scaling of the erosion curves to one, since decreased values of the suspension effect during the bedload event caused smaller total erosion predicted by the SA model.

Explicit consideration of the cover effect term $F_\mathrm{e}$ is recommended in the literature (e.g., Lamb et al., 2008a; Nelson and Seminara, 2011; Whipple et al., 2013). However, its influence appeared to be insignificant here. Given the site characteristics, the absence of the cover effect is plausible: immediately upstream of the instruments the channel is artificially constructed with a smooth steep bed, such that no sediment deposition occurs and detachment-limited conditions prevail (cf. Turowski et al., 2013; Beer et al., 2014).

Erosion rate c3i smoothly followed cumulated bedload transport $Q_{\mathrm{s,cum}}$ during the long period (cf. the evolution of the erosion gradient in Fig. 1c). This indicates that erosion is driven by particle impacts and that the dominant sediment effect is the tools effect at least here. A simple model in which the erosion rate is proportional to bedload transport rate $Q_\mathrm{s}$ (TO model) explains the data similarly well as other models incorporating the tools effect (Fig. 2, Table 2), including highly-developed mechanistic process models such as the full saltation-abrasion model (SA). The importance of the tools effect is in line with previous field and laboratory observations (Sklar and Dietrich, 2001; Turowski and Rickenmann, 2009; Cook et al., 2013; Wilson et al., 2013), and our data provide the first direct field evidence for the tools effect at the process scale (cf. Beer et al., 2014).

### 5.3 Optimized model parameters

For some of the models, the optimization procedure resulted in substantial improvements of their predictive power. Because of its large practical importance, we discuss the behaviour of the stream power incision model family (USP, EUSP) in detail and make some general remarks on the other models, especially those where we found large predictive difference between the common and the optimized parameters.

For the USP model, the optimized exponent $a_{\mathrm{USP\_o}}$ took the value of 1.5 for the long period and 1.1 for the bedload period (Table 2), reducing the deviation of the prediction from c3i. However, the choice of the exponent did not significantly affect the predictive power of the models (Fig. 3), at least when it remained within the range of values reported in the literature (between 0 and 2, see Lague, 2014, for a review). Moreover, the optimized parameter of the EUSP model $a_{\mathrm{EUSP\_o}} = 0.6$ is almost equal to the common value of $a_{\mathrm{EUSP\_c}} = 0.5$. However, our observations at the process scale are not directly comparable to previously published values, which were typically derived from measurements at the reach or catchment scale. A proper upscaling and a comparison with reach scale measurements would be necessary to give a complete interpretation of the results. Similar reasons as discussed in the section on model sensitivity can be cited to explain the slightly smaller predictive power of models USP and EUSP for the erosion period. For both models, we obtained optimized values of $a_{\mathrm{USP\_o}} = a_{\mathrm{EUSP\_o}} = 0.1$ in this period, but with no noticeable improvement over the common parameter of 0.5 (Fig. 3) as model performance remained at the levels of the common model versions. Thus, the inclusion of a threshold in the USP equation makes the common parameter value of 0.5 acceptable for the modelling of the general trend in the evolution of erosion, at least for the Erlenbach event discussed here.

The elimination of the cover term in the optimized versions of models LD and AB reduces these models to the models USP and EUSP respectively for the first two time periods. This confirms previous observations that the cover effect is generally negligible in the setting on hand. At the beginning of the erosion period there are the lowest values of the cover effect term observed (≥ 0.04; cf. Fig. 1c). Optimization lead to negative values of $c_{\mathrm{LD\_o}}$ and $c_{\mathrm{AB\_o}}$ resulting in comparably good performance of the two models, since the first "hump" in the c3i curve could be predicted. However, a negative exponent on the cover term contradicts the physical assumptions of the cover effect (see Appendix A) and rather is an emulation of the tools effect.

Optimizing models including the tools effect mainly resulted in reductions of the interquartile ranges of model deviations. Values for the long period and the bedload period were equally adjusted. Notable improvement, leading to a similar performance in comparison with the other models, was achieved in the SPP model, where the tools effect compensated the missing threshold of bedload motion. However, no model could clearly beat the performance of the TO model, a further indicator of the tools effect to be the dominant driver of bedrock erosion in our setup.

### 5.4 Generality of the results

Our results are site-specific and so far are only available for a single event using a mean sediment grain size. Nevertheless, they suggest that the excess stream power incision model, incorporating a threshold of bedload motion and a commonly used exponent of 0.5 (the EUSP model), can be used to reproduce tools-dominated incision if the details of erosional evolution within the events are not of interest. This would be the case for instance in long term, large scale landscape evolution studies.

For the USP model family at least some aspects of temporal upscaling are understood (e.g., Lague et al., 2005), but the situation so far is unclear for spatial upscaling in general, and for the temporal upscaling of sediment-flux-dependent incision models specifically (cf. Whipple and Tucker, 1999; Lague, 2010, 2014). Our data further highlight the prevalence of the tools effect in bedrock erosion at the process scale, indicating that erosion is driven by particle impacts (Sklar and Dietrich, 2004; Turowski et al., 2013). The cover effect and the threshold of suspension may be more important in streams with rough stream beds, varying sediment supply and located in tectonically active regions (cf. Sklar and Dietrich, 2006).

cc BY

## 6 Conclusions

Fluvial bedrock erosion is driven by the impacts of bedload particles, and out of several sediment effects, the tools effect dominantly determines erosion rates at the Erlenbach observatory. The pattern of transient erosion through the course of a single flood event can be described by a simple model in which erosion rate is proportional to cumulative bedload transport rate. Moreover, this simple model performs similarly well or better than more complex models from the literature, including the mechanistically-based saltation-abrasion model (Sklar and Dietrich, 2004), and several models from the stream-power incision model family. The model can be site-calibrated with temporally lumped data and is applicable in tools-dominated steep bedrock rivers, but also in e.g. bedload-exposed hydropower infrastructure.

On the scale of the individual event, models from the stream-power incision model family can adequately describe the general observed erosion trend. In our tests, the application of an excess shear stress model with an exponent of 0.5 does not capture the detailed evolution of erosion throughout the event, but is adequate to represent the overall form of the erosion curve. Analysis of further events is needed to constrain if this result is general, or whether it is specific to the event considered here. Additional data acquisition and analysis of transient erosion rates in other settings is required (Tucker and Whipple, 2002) to e.g. study interactions between different erosion processes that are not considered in modelling so far (Whipple et al., 2013) and potentially provide guidance for site-specific model choice based on the locally active morphological processes.

## Appendix A: Model selection

According to Sklar and Dietrich (2006) all fluvial bedrock incision models published so far can be represented by a generic equation (a detailed version of Eq. 1):

$$E = K\left(H_y - H_{y_c}\right)^a \left[1 - \left(\frac{u^*}{w_f}\right)^2\right]^b \left(1 - \frac{Q_s}{Q_{sc}}\right)^c Q_s^d \quad \text{(A1)}$$

Here $H_{yc}$ is a threshold term accounting for grain motion, $Q_{sc}$ is the sediment transport capacity, $u^*$ is flow shear velocity and $w_f$ is particle fall velocity in still water. The terms in brackets from the left to the right are the representatives of the bedload motion effect, the bedload suspension effect, the cover effect and the tools effect respectively (see Eq. 1).

Actually there are $2^4 = 16$ combinations of the four sediment effects controlled by the exponents *a*, *b*, *c* and *d* in an incision model that in turn can be adjusted for specific dominant erosion processes like abrasion, plucking and macroabrasion (Whipple et al., 2000; Sklar and Dietrich, 2004; Lamb et al., 2008; Chatanantavet and Parker, 2009; Dubinski and Wohl, 2013). We restricted our analysis to the eight model classes (i.e. combinations of sediment effect parameters) identified by Sklar and Dietrich (2006) that were proposed, analysed and applied in several studies to date, but added a simple bedload depended model (class Va). We analysed one representative of each bedrock incision model class whose selection and parametrization (Table 2) was based on the following reasons (cf. Sklar and Dietrich, 2006):

- Class I, unit stream power model (USP): this model (Seidl and Dietrich, 1992; Howard, 1994; Howard et al., 1994) is most widely used in landscape evolution modelling studies (Lague, 2014) and for the interpretation of channel long profiles (e.g., Braun and Willett, 2013), although there is evidence contradicting its predictions (Gasparini et al., 2007; Lague, 2014). It is straightforward since it only incorporates discharge data, neglecting any effects of sediments, and assumes $H_{yc} = 0$. The single exponent *a* to scale stream power (actually discharge) is mainly set to 0.5 in modelling studies as we did here, but may vary between 0 and 2 for field data (Croissant and Braun, 2014; Lague, 2014), while most field cases suggest $a = 1$ (e.g., Stock and Montgomery, 1999; Snyder et al., 2000; see Lague, 2014, for a review). The USP model is equivalent to the shear stress model (Howard and Kerby, 1983; Turowski, 2012) and their model exponents are related by a factor of 2/3 (Whipple and Tucker, 1999).

- Class II, excess unit stream power model (EUSP): an extended version of the USP model with non-zero $H_{yc}$ (Sklar and Dietrich, 2006), thus incorporating a threshold of unit stream power to permit grain motion. Here it was applied by setting the threshold of motion to the unit stream power at the observed inition of bedload transport ($\Omega = 407\,\mathrm{W\,m^{-2}}$) and with the same exponent $a = 0.5$ as in the USP model (e.g., Tucker and Slingerland, 1997; Whipple et al., 2000).

- Class III, linear decline model (LD): this model set was formulated by Whipple and Tucker (2002) and is functionally equivalent to the undercapacity model by Beaumont et al. (1992). However, the latter does not draw on the cover effect, but on consumption of discharge energy for sediment transport that would be used for erosion otherwise. Erosion rate is limited by the fraction of actual bedload $Q_s$ to bedload transport capacity $Q_{sc}$, i.e. the cover effect. If this fraction approaches 1 erosion decreases to 0 (Sklar and Dietrich, 2004). The exponential dependency of the cover term proposed by Turowski et al. (2007) was not applied due to the prevailing tools domain. We applied the bedload transport equation of Rickenmann (2001) to calculate $Q_{sc}$ with a prefactor calibrated for the Erlenbach, using a grain size fraction $d_{90}/d_{30}$ based on data by Rickenmann et al. (2012, Fig. 9). We restricted our analysis to the version of Whipple and Tucker (2002) with an exponent $a = 2$.

- Class IV, alluvial bedload (AB): Sklar and Dietrich (2006) proposed this version of the linear decline model LD, additionally accounting for the threshold of motion $H_{yc}$.

- Class Va, tools-only model (TO): this model simply relates erosion to the observed cumulative bedload $Q_{\mathrm{s,cum}}$ transport rate. We introduce it here with $d = 1$ and rank it into the classification of Sklar and Dietrich (2006) based on the top down introduction system of the sediment effects there.
- Class V, tools (T): the model of Foley (1980) was applied following the approximation given by Sklar and Dietrich (2006) using $a = -0.5$.
- Class VI, parabolic stream power (SPP): in their attempt to include both the tools and the cover effect, Whipple and Tucker (2002) developed this model based upon considerations of Sklar and Dietrich (1998). We chose the proposed version with $a = 1$.
- Class VII, saltation abrasion model without the suspension effect (SAws): the same model as SPP additionally incorporating the observed sediment motion threshold $H_{\mathrm{yc}}$, but by applying nondimensional excess shear stress instead of unit stream power.
- Class VIII, full saltation abrasion model (SA): the complete saltation abrasion model (Sklar and Dietrich, 2004) additionally accounts for the grain suspension effect. We adopted the threshold of ceasing erosion (1 in the suspension term, Eq. A1) from Sklar and Dietrich (2004), however this value is controversial (review e.g. by Cheng and Chiew, 1999), and indeed the whole conception has been questioned (Scheingross et al., 2014). The parameter $d$ responsible for the suspension term was set to 1.5 here, since this is consistent with the original model (cf. Sklar and Dietrich, 2004).

We did not apply the elaborate total-load model by Lamb et al. (2008) here due to its need for (i) high shear stress ratios (see above) and relative sediment supply to deviate from model SA (Lamb et al., 2008; Scheingross et al., 2014), and (ii) several required assumptions and iterations inserting additional uncertainties, so any result would not have been comparable. Models focusing on plucking as erosion process

(Chatanantavet and Parker, 2009; Dubinski and Wohl, 2013) were also not applied since abrasion can be assumed to be the dominant process in our experimental setting (cf. Beer et al., 2014).

## Appendix B: Detailed model results

The individual parameter sets of all incision models were optimized for the three time periods respectively (Table 2). In Fig. A1 a separate comparison of the transient behaviour is given for the particular model predictions to the observed erosion course c3i and the cumulative bedload transport $Q_{\mathrm{s,cum}}$.

*Acknowledgements.* The authors are grateful to Florian Heimann, James Kirchner, Colin Stark and Carlos Wyss for fruitful discussions and help with data analysis. Comments by Alexandre Badoux and Johannes Schneider on an earlier version greatly improved this article. This study was supported by SNF grant 200021_132163/1.

## References

Attal, M., Cowie, P. A., Whittaker, A. C., Hobley, D., Tucker, G. E., and Roberts, G. P.: Testing fluvial erosion models using the transient response of bedrock rivers to tectonic forcing in the Apennines, Italy, J. Geophys. Res., 116, F02005, doi:10.1029/2010JF001875, 2011.

Beaumont, C., Fullsack, P., and Hamilton, J.: Erosional control of active compressional orogens, in: Thrust tectonics, edited by McClay, K., Chapman and Hall, New York, 1–18, 1992.

Beer, A. R., Turowski, J. M., Fritschi, B., and Rieke-Zapp, D.: Field instrumentation for high-resolution parallel monitoring of bedrock erosion and bedload transport, Earth Surf. Proc. Land., early view, doi:10.1002/esp.3652, 2014.

Braun, J. and Willett, S. D.: A very efficient $O(n)$, implicit and parallel method to solve the stream power equation governing uvial incision and landscape evolution, Geomorphology, 180, 170–179, doi:10.1016/j.geomorph.2012.10.008, 2013.

Brent, R. P.: Algorithms for Minimization without Derivatives, Prentice-Hall, Englewood Cliffs, N. J., 1973.

Chatanantavet, P. and Parker, G.: Physically-based modeling of bedrock incision by abrasion, plucking, and macroabrasion, J. Geophys. Res., 114, F04018, doi:10.1029/2008JF001044, 2009.

Chatanantavet, P., Whipple, K. X., Adams, M. A., and Lamb, M. P.: Experimental study on coarse grain saltation dynamics in bedrock channels, J. Geophys. Res.-Earth, 118, 1161–1176, doi:10.1002/jgrf.20053, 2013.

Cheng, N. S. and Chiew, Y. M.: Analysis of initiation of sediment suspension from bed load, J. Hydraul. Eng.-ASCE, 125, 855–861, doi:10.1061/(ASCE)0733-9429(1999)125:8(855), 1999.

Croissant, T. and Braun, J.: Constraining the stream power law: a novel approach combining a landscape evolution model and an inversion method, Earth Surf. Dynam., 2, 155–166, doi:10.5194/esurf-2-155-2014, 2014.

Cook, K. L., Turowski, J. M., and Hovius, N.: A demonstration of the importance of bedload transport for fluvial bedrock erosion and knickpoint propagation: Earth Surf. Proc. Land., 38, 683–695, doi:10.1002/esp.3313, 2013.

Dubinski, I. M. and Wohl, E.: Relationships between block quarrying, bed shear stress, and stream power: a physical model of block quarrying of a jointed bedrock channel, Geomorphology, 180, 66–81, doi:10.1016/j.geomorph.2012.09.007, 2013.

Finnegan, N. J., Schumer, R., and Finnegan, S.: A signature of transience in bedrock river incision rates over timescales of 10(4)–10(7) years, Nature, 505, 391–394, doi:10.1038/nature12913, 2014.

Foley, M. G.: Bedrock incision by streams: summary, Geol. Soc. Am. Bull., Part II, 91, 2189–2213, doi:10.1130/0016-7606(1980)91<577:BIBSS>2.0.CO;2, 1980.

Gardner, T. W., Jorgensen, D. W., Shuman, C., and Lemieux, C. R.: Geomorphic and tectonic process rates – effects of measured time interval, Geology, 15, 259–261, doi:10.1130/0091-7613(1987)15<259:GATPRE>2.0.CO;2, 1987.

Gasparini, N. M., Whipple, K. X., and Bras, R. L.: Predictions of steady state and transient landscape morphology using sediment-flux-dependent river incision models, J. Geophys. Res., 112, F03S09, doi:10.1029/2006JF000567, 2007.

Gilbert, G. K.: Land sculpture, The Geology of the Henry Mountains, Chapter V, United States Department of the Interior, Washington, DC, 99–155, 1877.

cc BY

Goode, J. R. and Wohl, E.: Substrate controls on the longitudinal profile of bedrock channels: implications for reach-scale roughness, J. Geophys. Res.-Earth, 115, F03018, doi:10.1029/2008JF001188, 2010.

Hancock, G. S., Anderson, R. S., and Whipple, K. X.: Beyond power: bedrock river incision process and form, in: Rivers Over Rock: Fluvial Processes in Bedrock Channels, edited by: Tinkler, K. J. and Wohl, E. E., Geophysical Monograph, 107, American Geophysical Union, Washington, DC, 30–60, 1998.

Hartshorn, K., Hovius, N., Dade, W. B., and Slingerland, R. L.: Climate-driven bedrock incision in an active mountain belt, Science, 297, 2036–2038, doi:10.1126/science.1075078, 2002.

Howard, A. D.: A detachment-limited model of drainage basin evolution, Water Resour. Res., 30, 2261–2285, doi:10.1029/94WR00757, 1994.

Howard, A. D., Dietrich, W. E., and Seidl, M. A.: Modeling fluvial erosion on regional to continental scales, J. Geophys. Res., 99, 13971–13986, 1994.

Howard, A. D. and Kerby, G.: Channel changes in badlands, Geol. Soc. Am. Bull., 94, 739–752, doi:10.1130/0016-7606(1983)94<739:CCIB>2.0.CO;2, 1983.

Johnson, J. P. L., Whipple, K. X., Sklar, L. S., and Hanks, T. C.: Transport slopes, sediment cover, and bedrock channel incision in the Henry Mountains, Utah, J. Geophys. Res., 114, F02014, doi:10.1029/2007JF000862, 2009.

Lague, D.: The stream power river incision model: evidence, theory and beyond, Earth Surf. Proc. Land., 39, 38–61, doi:10.1002/esp.3462, 2014.

Lague, D., Crave, A., and Davy, P.: Laboratory experiments simulating the geomorphic response to tectonic uplift, J. Geophys. Res., 108, ETG3, doi:10.1029/2002JB001785, 2003.

Lague, D., Hovius, N., and Davy, P.: Discharge, discharge variability and the bedrock channel profile, J. Geophys. Res., 110, F04006, doi:10.1029/2004JF000259, 2005.

Lamb, M. P., Dietrich, W. E., and Sklar, L. S.: A model for fluvial bedrock incision by impacting suspended and bed load sediment, J. Geophys. Res., 113, F03025, doi:10.1029/2007JF000915, 2008a.

Lamb, M. P., Dietrich, W. E., and Venditti, J. G.: Is the critical Shields stress for incipient sediment motion dependent on channel-bed slope?, J. Geophys. Res., 113, F02008, doi:10.1029/2007JF000831, 2008b.

Mills, H. H.: Apparent increasing rates of stream incision in the eastern united states during the late cenozoic, Geology, 28, 955–957, doi:10.1130/0091-7613(2000)28<955:AIROSI>2.0.CO;2, 2000.

cc BY

Nelder, J. A. and Mead, R.: A simplex-method for function minimization, Comput. J., 7, 308–313, 1965.

Nelson, P. A. and Seminara, G.: Modeling the evolution of bedrock channel shape with erosion from saltating bed load, Geophys. Res. Lett., 38, L17406, doi:10.1029/2011GL048628, 2011.

Rickenmann, D.: Comparison of bed load transport in torrent and gravel bed streams, Water Resour. Res., 37, 3295–3305, doi:10.1029/2001WR000319, 2001.

Rickenmann, D., Turowski, J. M., Fritschi, B., Klaiber, A., and Ludwig, A.: Bedload transport measurements at the erlenbach stream with geophones and automated basket samplers, Earth Surf. Proc. Land., 37, 1000–1011, doi:10.1002/esp.3225, 2012.

Rieke-Zapp, D. H., Beer, A., Turowski, J. M., and Campana, L.: IN SITU MEASUREMENT OF BEDROCK EROSION, Int. Arch. Photogramm. Remote Sens. Spatial Inf. Sci., XXXIX-B5, 429–433, doi:10.5194/isprsarchives-XXXIX-B5-429-2012, 2012.

Scheingross, J. S., Brun, F., Lo, D. Y., Omerdin, K., and Lamb, M. P.: Experimental evidence for fluvial bedrock incision by suspended and bedload sediment, Geology, 42, 523–526, doi:10.1130/G35432.1, 2014.

Seidl, M. A. and Dietrich, W. E.: The problem of channel erosion into bedrock, Catena Supplement, 23, 101–124, 1992.

Seidl, M. A., Dietrich, W. E., and Kirchner, J. W.: Longitudinal profile development into bedrock: an analysis of Hawaiian channels, J. Geol., 102, 457–474, 1994.

Sklar, L. S. and Dietrich, W. E.: Sediment and rock strength controls on river incision into bedrock, Geology, 29, 1087–1090, doi:10.1130/0091-7613(2001)029<1087:SARSCO>2.0.CO;2, 2001.

Sklar, L. S. and Dietrich, W. E.: A mechanistic model for river incision into bedrock by saltating bed load, Water Resour. Res., 40, W06301, doi:10.1029/2003WR002496, 2004.

Sklar, L. S. and Dietrich, W. E.: The role of sediment in controlling steady-state bedrock channel slope: implications of the saltation-abrasion incision model, Geomorphology, 82, 58–83, doi:10.1016/j.geomorph.2005.08.019, 2006.

Snyder, N. P., Whipple, K. X., Tucker, G. E., and Merritts, D. J.: Landscape response to tectonic forcing: digital elevation model analysis of stream proles in the Mendocino triple junction region, northern California, Geol. Soc. Am. Bull., 112, 1250–1263, 2000.

CC BY

Snyder, N. P., Whipple, K. X., Tucker, G. E., and Merritts, D. J.: Importance of a stochastic distribution of floods and erosion thresholds in the bedrock river incision problem, J. Geophys. Res., 108, 2117, doi:10.1029/2001JB001655, 2003.

Stock, J. D. and Montgomery, D. R.: Geologic constraints on bedrock river incision using the stream power law, J. Geophys. Res., 104, 4983–4993, doi:10.1029/98JB02139, 1999.

Tomkin, J. H., Brandon, M. T., Pazzaglia, F. J., Barbour, J. R., and Willett, S. D.: Quantitative testing of bedrock incision models for the clearwater river, nw, washington state, J. Geophys. Res., 108, 2308, doi:10.1029/2001JB000862, 2003.

Tucker, G. E. and Slingerland, R. L.: Drainage basin response to climate change, Water Resour. Res., 33, 2031–2047, doi:10.1029/97WR00409, 1997.

Tucker, G. E. and Whipple, K. X.: Topographic Outcomes predicted by stream erosion models: sensitivity analysis and intermodel comparison, J. Geophys. Res., 107, 2179–2194, doi:10.1029/2001JB000162, 2002.

Turowski, J. M.: Semi-alluvial channels and sediment-flux-driven bedrock erosion, in: Gravel Bed Rivers: Processes, Tools, Environments,Chap. 29, edited by: Church, M., Biron, P., and Roy, A., John Wiley and Sons, Chichester, 401–416, doi:10.1002/9781119952497, 2012.

Turowski, J. M. and Rickenmann, D.: Tools and cover effects in bedload transport observations in the Pitzbach, Austria, Earth Surf. Process. Landforms, 34, 26–37, doi:10.1002/esp.1686, 2009.

Turowski, J. M., Lague, D., and Hovius, N.: Cover effect in bedrock abrasion: a new derivation and its implication for the modeling of bedrock channel morphology, J. Geophys. Res., 112, F04006, doi:10.1029/2006JF000697, 2007.

Turowski, J. M., Hovius, N., Hsieh, M. L., Lague, D., and Chen, M. C.: Distribution of erosion across bedrock channels, Earth Surf. Process. Landforms, 33, 353–363, doi:10.1002/esp.1559, 2008.

Turowski, J. M., Boeckli, M., Rickenmann, D., and Beer, A. R.: Field measurements of the energy delivered to the channel bed by moving bedload and links to bedrock erosion, J. Geophys. Res., 118, 2438–2450, doi:10.1002/2013JF002765, 2013.

Valla, P. G., van der Beek, P. A., and Lague, D.: Fluvial incision into bedrock: insights from morphometric analysis and numerical modeling of gorges incising glacial hanging valleys (western alps, france), J. Geophys. Res.-Earth, 115, F02010, doi:10.1029/2008JF001079, 2010.

cc BY

van der Beek, P. and Bishop, P.: Cenozoic river profile development in the upper Lachlan catchment (SE Australia) as a test of quantitative fluvial incision models, J. Geophys. Res., 108, 2309, doi:10.1029/2002JB002125, 2003.

Whipple, K. X.: Bedrock rivers and the geomorphology of active orogens, Annu. Rev. Earth Planet. Sci., 32, 151–185, doi:10.1146/annurev.earth.32.101802.120356, 2004.

Whipple, K. X. and Tucker, G. E.: Dynamics of the stream-power river incision model: implications for height limits of mountain ranges, landscape response timescales, and research needs, J. Geophys. Res., 104, 17661–17674, doi:10.1029/1999JB900120, 1999.

Whipple, K. X. and Tucker, G. E.: Implications of sediment-flux-dependent river incision models for landscape evolution, J. Geophys. Res., 107, 2039, doi:10.1029/2000JB000044, 2002.

Whipple, K. X., Hancock, G. S., and Anderson, R. S.: River incision into bedrock: mechanics and relative efficacy of plucking, abrasion, and cavitation, Geol. Soc. Am. Bull., 112, 490–503, doi:10.1130/0016-7606(2000)112<0490:RIIBMA>2.3.CO;2, 2000.

Whipple, K. X., DiBiase, R. A., and Crosby, B. T.: Bedrock rivers, in: Treatise in Geomorphology, Methods in Geomorphology, 9.28, edited by: Switzer, A. and Kennedy, D. M., Elsevier, Amsterdam, 550–573, 2013.

Wilson, A., Hovius, N., and Turowski, J. M.: Upstream facing convex surfaces: bedrock bedforms produced by fluvial bedload abrasion, Geomorphology, 180/181, 187–204, doi:10.1016/j.geomorph.2012.10.010, 2013.

Wohl, E. E.: Bedrock channel morphology in relation to erosional processes, in: Rivers Over Rock: Fluvial Processes in Bedrock Channels, edited by: Tinkler, K. J. and Wohl, E. E., Geophysical Monograph, 107, American Geophysical Union, Washington, DC, 133–151, 1998.

cc BY

CC BY

**Table 1.** List of applied incision models (see Appendix A for detailed explanations). The horizontal line subdivides models that include the tools effect from models that do not.

| model class[a] | model name[a] | original reference | considered sediment effects[c] motion | susp. | cover | tools |
|---|---|---|---|---|---|---|
| I | unit stream power (USP) | Howard et al. (1994) | – | – | – | – |
| II | excess unit stream power (EUSP) | Sklar and Dietrich (2006) | √ | – | – | – |
| III | linear decline (LD) | Whipple and Tucker (2002) | – | – | √ | – |
| IV | alluvial bedload (AB) | Sklar and Dietrich (2006) | √ | – | √ | – |
| Va | tools only (TO)[b] | this work | – | – | – | √ |
| V | tools (T) | Foley (1980) | √ | – | – | √ |
| VI | parabolic stream power (SPP) | Whipple and Tucker (2002) | – | – | √ | √ |
| VII | saltation-abrasion without suspension (SAws) | Sklar and Dietrich (2006) | √ | – | √ | √ |
| VIII | saltation-abrasion (SA) | Sklar and Dietrich (2004) | √ | √ | √ | √ |

[a] Based on the classification by Sklar and Dietrich (2006); model choice and description is given in the Appendix A.

[b] Concept of this work.

[c] Grain motion and suspension thresholds, cover and tools effects.

**Table 2.** Exponents of the four sediment effects for the common (com) and optimized (opt) model versions respectively, given for the three time periods of consideration and resulting model performance relating to c3i. Implausible parameters are attenuated bold and model groups with and without the tools effect are separated by a horizontal line.

| model period | model name[a] | applied model parameters[b] | | | | | | | | model performance | |
|---|---|---|---|---|---|---|---|---|---|---|---|
| | | motion | | suspension | | cover | | tools | | | |
| | | a_com | a_opt | b_com | b_opt | c_com | c_opt | d_com | d_opt | RMSE_c [%] | RMSE_o [%] |
| long period | USP (class I) | 0.5[c] | 1.5[c] | – | – | – | – | – | – | 10 | 8 |
| | EUSP (class II) | 0.5 | 0.6 | – | – | – | – | – | – | 7 | 7 |
| | LD (class III) | 2.0[c] | 1.5[c] | – | – | 1.0 | 0.0 | – | – | 10 | 8 |
| | AB (class IV) | 1.5 | 0.6 | – | – | 1.0 | 0.0 | – | – | 10 | 7 |
| | TO (class Va) | – | – | – | – | – | – | 1.0 | 1.0 | 3 | 3 |
| | T (class V) | −0.5 | 0.3 | – | – | – | – | 1.0 | 1.0 | 5 | 3 |
| | SPP (class VI) | 1.0[c] | −1.1[c] | – | – | 1.0 | 1.3 | 1.0 | 1.6 | 7 | 3 |
| | SAws (class VII) | −0.5 | −0.5 | – | – | 1.0 | 0.9 | 1.0 | 1.4 | 4 | 3 |
| | SA (class VIII) | −0.5 | **13** | 1.5 | **20** | 1.0 | 0.6 | 1.0 | 1.1 | 6 | 3 |
| bedload period | USP (class I) | 0.5[c] | 1.1[c] | – | – | – | – | – | – | 9 | 8 |
| | EUSP (class II) | 0.5 | 0.6 | – | – | – | – | – | – | 8 | 8 |
| | LD (class III) | 2.0[c] | 1.0[c] | – | – | 1.0 | 0.0 | – | – | 10 | 8 |
| | AB (class IV) | 1.5 | 0.6 | – | – | 1.0 | 0.0 | – | – | 11 | 8 |
| | TO (class Va) | – | – | – | – | – | – | 1.0 | 1.0 | 4 | 4 |
| | T (class V) | −0.5 | 0.3 | – | – | – | – | 1.0 | 1.0 | 6 | 4 |
| | SPP (class VI) | 1.0[c] | −1.1[c] | – | – | 1.0 | 1.3 | 1.0 | 1.6 | 7 | 4 |
| | SAws (class VII) | −0.5 | −0.5 | – | – | 1.0 | 0.9 | 1.0 | 1.4 | 4 | 4 |
| | SA (class VIII) | −0.5 | **13** | 1.5 | **20** | 1.0 | 0.6 | 1.0 | 1.1 | 6 | 3 |
| erosion period | USP (class I) | 0.5[c] | 0.1[c] | – | – | – | – | – | – | 11 | 11 |
| | EUSP (class II) | 0.5 | 0.1 | – | – | – | – | – | – | 11 | 11 |
| | LD (class III) | 2.0[c] | 2.5[c] | – | – | 1.0 | −1.4 | – | – | 14 | 6 |
| | AB (class IV) | 1.5 | 1.7 | – | – | 1.0 | −1.4 | – | – | 14 | 6 |
| | TO (class Va) | – | – | – | – | – | – | 1.0 | 1.9 | 7 | 5 |
| | T (class V) | −0.5 | −0.1 | – | – | – | – | 1.0 | 1.6 | 6 | 5 |
| | SPP (class VI) | 1.0[c] | −1.5[c] | – | – | 1.0 | 0.0 | 1.0 | 1.5 | 12 | 3 |
| | SAws (class VII) | −0.5 | −2.4 | – | – | 1.0 | 2.6 | 1.0 | 2.6 | 8 | 5 |
| | SA (class VIII) | −0.5 | **13** | 1.5 | **20** | 1.0 | 0.1 | 1.0 | 0.1 | 7 | 4 |

[a] Denotations given in Table 1.

[b] Respective parameters for commonly used (_com) and optimized (_opt) values applied for the four sediment effects.

[c] This exponent is used for entire stream power neglecting the grain motion threshold effect.

cc BY

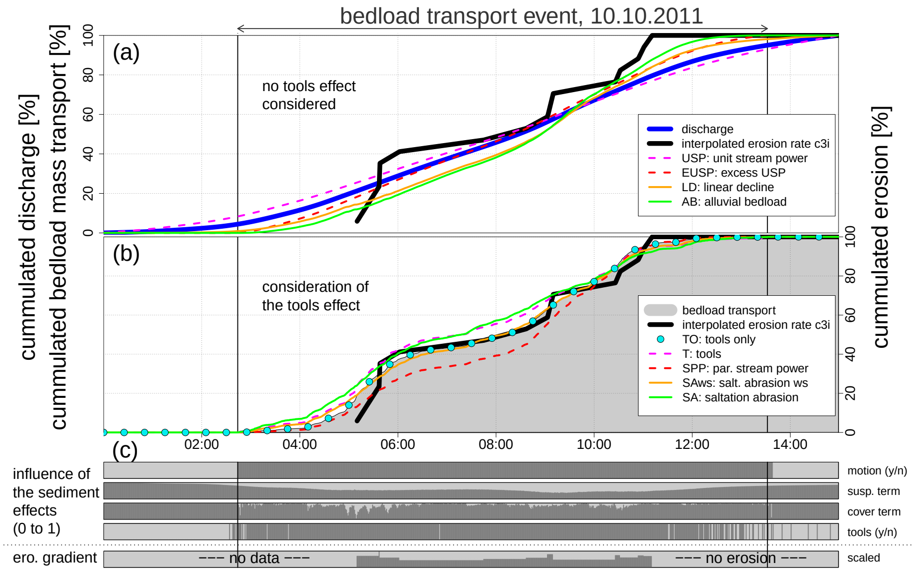

**Figure 1.** Evolution of the modelled erosion signals over the flood event compared to discharge, bedload mass transport and interpolated erosion rate (see Table 1 and Appendix A for model descriptions) given for the long period. **(a)** Scaled predictions of models neglecting the tools effect (models USP until AB), **(b)** scaled predictions for models incorporating the tools effect (models TO until SA) and **(c)** the transient evolution of the four sediment effects (factors in Eq. 1) and the gradient of the erosion curve c3i (the data resolution is in minutes). Note that the threshold of motion term and the tools term are binary, but the suspension term, the cover term and the erosion gradient can continuously vary between 0 and 1; see text for further explanations.

Title Page
Abstract | Introduction
Conclusions | References
Tables | Figures
◀| |▶
◀ ▶
Back | Close
Full Screen / Esc
Printer-friendly Version
Interactive Discussion

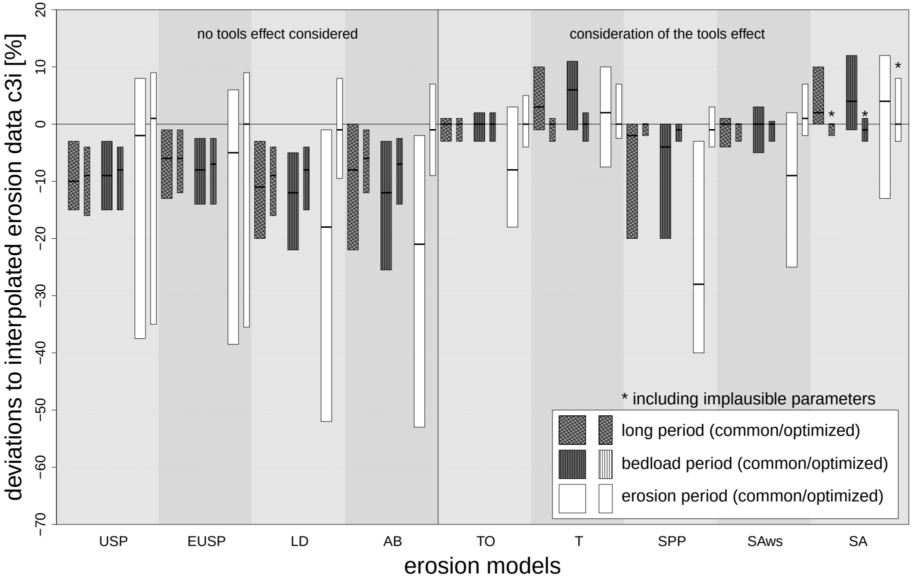

**Figure 2.** Comparison of model prediction deviations from the course of bedrock erosion c3i. Each model performance is given for the three different periods of consideration (different illustration patterns) with runs using both common and optimised parameter sets (wide and narrow boxes) respectively. For model denotations see Table 1.

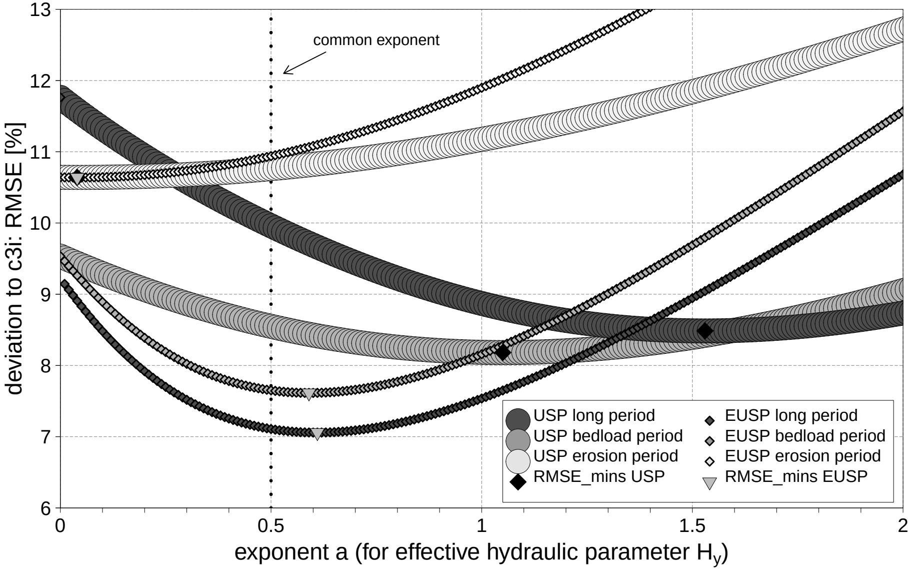

**Figure 3.** Performance of the USP and EUSP models as RMSE deviation to c3i given for the common range of the stream power exponents *a* (steps of 0.1; see Eq. 1) for the three time periods. The dotted vertical line indicate the commonly used exponent; the diamonds and the triangles show optimized parameters.

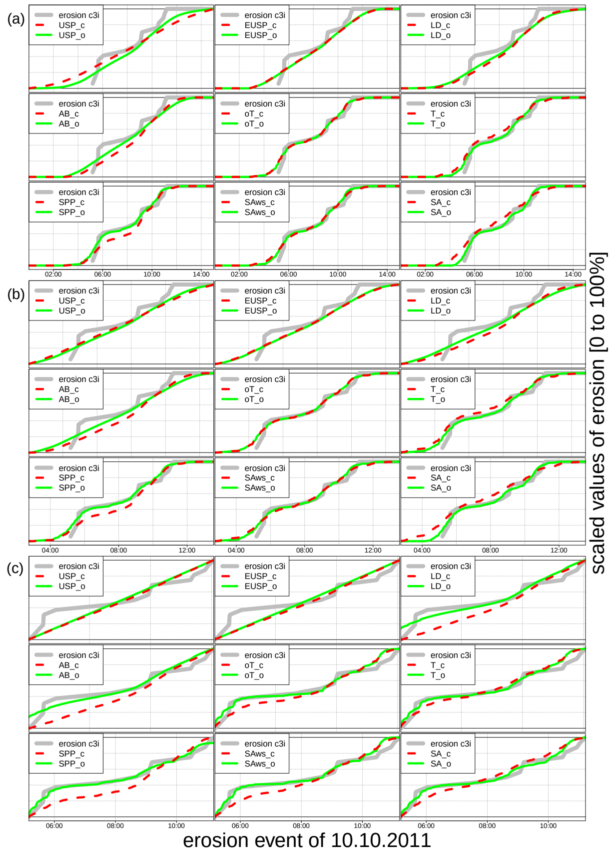

**Figure A1.** Separate comparison of each of the model-based erosion predictions to c3i for **(a)** the long period, **(b)** the bedload period and **(c)** the erosion period using the individual common and optimized parameter sets respectively.